A CENTERED DFT-BASED DISCRETE FRACTIONAL FOURIER TRANSFORM AND ITS APPLICATION TO CHIRP SIGNAL PARAMETER ESTIMATION

Ahmet Serbes[1] *and Lutfiye Durak*[2]

Department of Electronics and Communications Engineering, Yildiz Technical University,
Yildiz, Besiktas, 34349, Istanbul, Turkey, phone: + (90) 212-383-2490
[1]aserbes@yildiz.edu.tr, [2]lutfiye@ieee.org

ABSTRACT

We propose a new discrete fractional Fourier transform (DFrFT) scheme based on eigentransforms of the centered DFT matrix and present its application to chirp parameter estimation problem. We show that eigentransforms of the centered DFT provides a simple and straightforward method in the derivation of the centered DFrFT matrix. The method makes use of Gram-Schmidt orthogonalization algorithm to refine the eigenvectors that are employed in the DFrFT matrix computation. The simulation results show how the proposed DFrFT mimics its continuous counterpart and finally an application on chirp rate estimation is presented .

1. INTRODUCTION

The fractional Fourier transform (FrFT) has found many applications in various areas including signal processing [1], time-frequency analysis [2], quantum mechanics [3], and signal recovery [4]. FrFT is a potentially powerful tool in the analysis of chirp-type signals. As chirp signals are widely used in radar, sonar and communication systems, estimation of their parameters such as amplitude, chirp rate, initial frequency and initial phase is an important problem [5].

In recent years, so many efforts have been invested in obtaining the discrete Fractional Fourier transform (DFrFT) that inherits the properties of the continuous FrFT [6]. Early works on DFrFT can be split into two major groups. The first approach is based on an $\mathbf{S}$ matrix introduced by Dickinson *et al.* [7] which is an almost-tridiagonal matrix commuting with the DFT matrix. In this approach, the eigenvectors of the $\mathbf{S}$ matrix are shown to be discrete Hermite-Gauss-like functions [8, 9].

The second approach is based on an exact-tridiagonal Grünbaum [10] matrix, which is employed in combination with the $\mathbf{S}$ matrix to furnish a basis of eigenvectors for the DFrFT matrix [11]. Both of the approaches are approximations for the Hermite-Gauss eigenvectors of the DFT matrix.

In this work we introduce a different approach to derive the DFrFT matrix, which mimics the properties of the continuous FrFT. Using a simple and straightforward derivation of the eigenvectors of the DFT matrix, we employ a Gram-Schmidt based orthogonalization algorithm to find orthonormal eigenvectors. The N-point centered discrete Fourier transform (CDFT) matrix $\mathbf{W_N}$ is defined as a unitary matrix whose elements are,

$$(\mathbf{W_N})_{n,m} = \frac{1}{\sqrt{N}} \exp\left(-j\frac{2\pi}{N}(n-c)(m-c)\right), \quad n,m = 0,1,...,N-1; \quad c = \frac{N-1}{2}. \tag{1}$$

If the Fourier transform of $f(u)$ is $F(u)$, then Fourier transform of $F(u)$ is $f(-u)$. Applying the Fourier transform to $f(-u)$ yields $F(-u)$. Finally, taking one more Fourier transform will produce $f(u)$ again. Analogous to its continuous counterpart the CDFT matrix satisfies,

$$\mathbf{W}_N^4 = \mathbf{I}_N. \tag{2}$$

where $\mathbf{I}_N$ is the identity matrix of order N. As four consecutive DFT operations correspond to the identity transform, the CDFT matrix has four distinct eigenvalues $\lambda \in \{1, -j, -1, j\}$ [13]. The DFT matrix is a symmetric Hermitian matrix. Thus, using the eigenvalue decomposition, $\mathbf{W}_N$ can be written in the form of

$$\mathbf{W}_N = \mathbf{U}_N \mathbf{\Lambda}_N \mathbf{U}_N^T \tag{3}$$

where, $(.)^T$ is the transpose operator, $\mathbf{U}$ is the real Hermite eigenvectors of the CDFT matrix and $\mathbf{\Lambda}$ is the diagonal matrix containing the corresponding eigenvalues. As the continuous-time FrFT is a generalization of the Fourier transform (FT) with an order parameter a, $a \in [0, 4]$, we generalize the eigenvalue-decomposition-type FT expression into discrete FrFT by taking the a^{th} fractional power of $\mathbf{W}_N$ matrix. We form the centered discrete FrFT (CDFrFT) matrix and use it in the chirp-rate estimation application.

2. PRELIMINARIES

We define the continuous FrFT and give some of its properties in the following.

Definition: The a^{th}-order continuous FrFT is defined as a linear operator acting on an integrable function $f(u)$ for $0 < a < 4$:

$$f_a(u') = \sqrt{1 - j\cot(\alpha)} \int_{-\infty}^{\infty} f(u) exp\Big(i\pi\big(\cot(\alpha)u^2 - 2\csc(\alpha)uu' + cot(\alpha)u'^2\big)\Big)\mathrm{d}u, \tag{4}$$

where $\alpha = a\pi/2$ is the transformation angle. The continuous FrFT kernel turns into the ordinary continuous FT kernel for $\alpha = \pi/2$. For $\alpha = 0$, the kernel is the identity operator.

The authors are supported by the Scientific and Technological Research Council of Turkey, TUBITAK under the grant of Project No. 105E078.

Properties of the FrFT: The continuous FrFT is a unitary transform that satisfies index additivity property. Consecutive FrFT of a function f with $\mathscr{F}^{a_1}[\mathscr{F}^{a_2}[...\mathscr{F}^{a_k}]...]](f)(u)$ is equal to taking only one FrFT of the function with order $\mathscr{F}^{a_1+a_2+...+a_k}(f)(u)$.

One of the most important features of the continuous FrFT is the rotation property in time-frequency axis. The FrFT rotates the time-frequency axis with an angle proportional to the FrFT order. The rotation angle is $\alpha = a\pi/2$, where a is the FrFT order. This property can be thought as rotating the axis of Wigner distribution (WD) $W_f(u,u')$ of $f(u)$ counter-clockwise,

$$W_{f_a}(u,u') = W_f(u\cos\alpha - u'\sin\alpha, u\sin\alpha + u'cos\alpha) \quad (5)$$

where W_{f_a} is the WD of the a^{th}-order FrFT of $f(u)$.

The squared magnitude of $f_a(u)$ is equal to the integral projection of the WD of $f(u)$ onto the axis making angle α with the u-axis. Let $\mathscr{R}_\alpha$ be the integral projection (or the Radon transform) operator, which takes the integral projection of $W(u,u')$ onto the rotated axis making angle α with the u-axis. It is possible to express

$$\mathscr{R}_\alpha(W_f(u,u')) = |f_a(u)|^2. \quad (6)$$

When $a = 1$, the Radon transform by the angle $\alpha = \pi/2$ gives us the squared magnitude of the FT of the signal.

As FrFT reduces to the ordinary FT when $a = 1$, the DFrFT matrix of order $a = 1$ should reduce to the ordinary DFT matrix in the discrete case. The DFrFT is desired to mimic at least unitary, index additivity and rotation properties by approximating the samples of the continuous FrFT.

3. EIGENANALYSIS OF THE CDFT MATRIX

The DFT maps the samples of $f[n]$, $n = 1,2,...,N-1$ to $[0,\ 2\pi]$ discrete frequency space with an interval $2\pi/N$, whereas the CDFT maps to $[-\pi,\ \pi]$ space assuming $n = -(N-1)/2,...,(N-1)/2$. Therefore, contrary to the DFT, the CDFT allows to define even and odd functions, i.e, Hermite-Gauss functions that are eigenfunctions of the continuous FrFT. In order to approximate the samples of the continuous FrFT and to imply the rotation property, Hermite-Gauss eigenvectors of the DFT matrix has to be obtained. The reason we have used the CDFT matrix instead of the ordinary DFT matrix is that, the Hermite-Gauss functions are eigenvectors of *only* the CDFT matrix, not the DFT matrix. In the eigenanalysis of the CDFT matrix, let us determine the matrices that include the eigenvectors of $\mathbf{W}_N$ explicitly by the following theorem.

Theorem: The Hermite-Gauss-like eigenvector matrices of the CDFT matrix is,

$$\mathbf{V}_1 = \frac{1}{2}\left(\Re\{\mathbf{W}_N\} + (\Re\{\mathbf{W}_N\})^2\right) \quad (7a)$$

$$\mathbf{V}_2 = \frac{1}{2}\left(\Re\{\mathbf{W}_N\} - (\Re\{\mathbf{W}_N\})^2\right) \quad (7b)$$

$$\mathbf{V}_3 = \frac{1}{2}\left(\Im\{\mathbf{W}_N\} + (\Im\{\mathbf{W}_N\})^2\right) \quad (7c)$$

$$\mathbf{V}_4 = \frac{1}{2}\left(\Im\{\mathbf{W}_N\} - (\Im\{\mathbf{W}_N\})^2\right) \quad (7d)$$

where, $\mathbf{V}_1$, $\mathbf{V}_2$, $\mathbf{V}_3$, and $\mathbf{V}_4$ are eigenvectors associated with eigenvalues 1, -1, j, and $-j$, respectively. $\Re$ and $\Im$ denote the real and imaginary parts, and $\mathbf{W}_N$ is the CDFT matrix as defined in (1).

Proof: Re-arranging (2) as $\mathbf{W}_N^4 - \mathbf{I}_N = 0$ and rewriting it in its factored form as

$$(\mathbf{W}_N - \mathbf{I}_N)(\mathbf{W}_N + \mathbf{I}_N)(\mathbf{W}_N - j\mathbf{I}_N)(\mathbf{W}_N + j\mathbf{I}_N) = 0 \quad (8)$$

leads us to a very important result when rewritten in four different eigenequation forms for the DFT as stated earlier by Bose [13]. As for the eigenvalues associated with $\lambda = 1$, we obtain

$$(\mathbf{W}_N - \mathbf{I}_N)(\mathbf{W}_N^3 + \mathbf{W}_N^2 + \mathbf{W}_N + \mathbf{I}_N) = 0 \quad (9)$$

with the corresponding eigenvector,

$$\mathbf{V}_1 = (\mathbf{W}_N^3 + \mathbf{W}_N^2 + \mathbf{W}_N + \mathbf{I}_N) \quad (10a)$$

which satisfies $\mathbf{W}_N\mathbf{V}_1 = \mathbf{V}_1$. The other eigenvectors can be obtained in the same manner,

$$\mathbf{V}_2 = (\mathbf{W}_N^3 - \mathbf{W}_N^2 + \mathbf{W}_N - \mathbf{I}_N) \quad (10b)$$

$$\mathbf{V}_3 = (\mathbf{W}_N^3 + j\mathbf{W}_N^2 - \mathbf{W}_N - j\mathbf{I}_N) \quad (10c)$$

$$\mathbf{V}_4 = (\mathbf{W}_N^3 - j\mathbf{W}_N^2 - \mathbf{W}_N + j\mathbf{I}_N) \quad (10d)$$

The eigenvectors are obtained by summing four unitary matrices and therefore they have eigenvalues of modulus 4. Note that $\mathbf{V}_1$ and $\mathbf{V}_2$ are pure real and $\mathbf{V}_3$ and $\mathbf{V}_4$ are pure imaginary, since $\mathbf{W}_N^3 + \mathbf{W}_N$ and $\mathbf{W}_N^2$ are pure real and $\mathbf{W}_N^3 - \mathbf{W}_N$ is pure imaginary

$$\mathbf{W}_N{}^3 + \mathbf{W}_N = 2\Re\{\mathbf{W}_N\} \quad (11a)$$

$$\mathbf{W}_N{}^3 - \mathbf{W}_N = -2j\Im\{\mathbf{W}_N\} \quad (11b)$$

$$\mathbf{W}_N{}^2 + \mathbf{I}_N = 2(\Re\{\mathbf{W}_N\})^2 \quad (11c)$$

$$\mathbf{W}_N{}^2 - \mathbf{I}_N = -2(\Im\{\mathbf{W}_N\})^2. \quad (11d)$$

Substituting appropriate terms in (10) with (11), we obtain

$$\mathbf{V}_1 = 2\left(\Re\{\mathbf{W}_N\} + (\Re\{\mathbf{W}_N\})^2\right), \quad (12a)$$

$$\mathbf{V}_2 = 2\left(\Re\{\mathbf{W}_N\} - (\Re\{\mathbf{W}_N\})^2\right), \quad (12b)$$

$$\mathbf{V}_3 = -2j\left(\Im\{\mathbf{W}_N\} + (\Im\{\mathbf{W}_N\})^2\right), \quad (12c)$$

$$\mathbf{V}_4 = -2j\left(\Im\{\mathbf{W}_N\} - (\Im\{\mathbf{W}_N\})^2\right). \quad (12d)$$

These equations do not satisfy (3), since Hermite-like eigenvectors have to be real and unitary. In order to obtain real and unitary eigenvectors, we divide $\mathbf{V}_1$ and $\mathbf{V}_2$ by 4, and $\mathbf{V}_3$ and $\mathbf{V}_4$ by $-4j$, since these eigenvectors have eigenvalues of modulus 4. The proof is complete. □

Notice that all $\mathbf{V}_i$, $i = 1,2,3,4$ are commuting with the CDFT matrix and therefore have the eigenvectors divided into four multiplicities. The acquired eigenvectors $\mathbf{V}_i$, are employed in the calculation of the DFrFT matrix, in the following section.

4. OBTAINING CENTERED-DFRFT MATRIX

The FrFT operator of order a can be defined as the a^{th} power of the ordinary DFT operator $\mathbf{W}_N$. Hence, the DFrFT matrix can be expressed by

$$\mathbf{W}_N^a = \mathbf{U}_N\mathbf{\Lambda}_N^a\mathbf{U}_N^T \quad (13)$$

Table 1: Multiplicities of the eigenvalues of the $N \times N$ CDFT matrix [12].

N	1	j	-1	j
4m	m	m	m	m
4m+1	m+1	m	m	m
4m+2	m+1	m+1	m	m
4m+3	m+1	m+1	m+1	m

where $\mathbf{\Lambda}_N^a$ is explicitly [12],

$$\mathbf{\Lambda}_N^a = diag(e^{-j0}, e^{-j\frac{\pi}{2}a}, \ldots, e^{-j\frac{\pi}{2}a(N-2)}, e^{-j\frac{\pi}{2}a(N-1)}) \quad (14)$$

The multiplicities of the eigenvalues of the CDFT matrix are given in Table 1.

The columns of the matrices stated in (7) are not linearly independent, since they are not full rank. An easy and quick way to obtain the linearly independent and orthonormal columns of them is to compute the reduced echelon form of these matrices, pick only the columns associated with the pivots and employ an orthogonalization algorithm, i.e., Gram-Schmidt orthogonalization (GSO) algorithm.

We have employed Gauss-Jordan elimination method to find the pivots and chosen the linearly independent columns, therefore throwing away some columns for each $\mathbf{V}_i$, $i = \{1,2,3,4\}$. Then, we have employed the celebrated modified GSO (m-GSO) [14] algorithm to obtain the normalized linearly independent orthonormal eigenvectors.

Recall that the reason of employing CDFT matrix is that, discrete Hermite-Gauss functions are eigenvectors of the CDFT matrix, but the eigenvectors of DFT matrix is phase-shifted version of the discrete Hermite-Gauss functions. Applying the same method directly to the DFT matrix will produce incorrect results. When a discrete Hermite function is transformed using the DFT matrix, the result is not a discrete Hermite function, rather it is a shifted version of the Hermite function modulated by a complex sinusoidal.

4.1 Modified Gram-Schmidt Algorithm

The Hermite-like orthogonal CDFT eigenvectors can be obtained by employing the m-GSO. Let

- $\mathbf{y}$: non-orthonormal columns of $\mathbf{V}_i$ after Gauss-Jordan elimination. (There are k_i columns for each $\mathbf{V}_i$.)
- $\bar{\mathbf{v}}$: orthonormal columns obtained by m-GSO
- k_i: number of pivots in $\mathbf{V}_i$,

then for each $\mathbf{V}_i$ the algorithm is summarized as follows.

for $n = 1$ to k_i

for $m = 1$ to n

$$\mathbf{y}_n = \mathbf{y}_n - \frac{<\mathbf{y}_m, \mathbf{y}_n>}{<\mathbf{y}_m, \mathbf{y}_m>}\mathbf{y}_m$$

end

$$\bar{\mathbf{v}}_n = \frac{\mathbf{y}_n}{||\mathbf{y}_n||}$$

end

where $<.>$ is an inner product. The m-GSO algorithm normalizes any set of vectors by using projection and subtraction. In the end, normalization operators make the orthonormal components remain only. In the first step, a vector is taken and the projections of the remaining vectors are subtracted from the vector, following a normalization step. The process is completed when this operation is carried for all vectors.

4.2 The Centered-DFrFT Matrix

Let $\bar{\mathbf{V}}_i$, $i = 1,2,3,4$ be the new linearly independent orthonormal eigenvector set after m-GSO algorithm. The size of the new eigenvectors $\bar{\mathbf{V}}_i$ is $N \times k_i$, where k_i is the rank of $\mathbf{V}_i$, which is already at hand after Gauss-Jordan elimination process. k_i can also be calculated by referring to the multiplicities of eigenvalues, which is shown in Table 1.

The ordinary CDFT matrix can be obtained by calculating the sum of four eigenvalue decompositions of $\bar{\mathbf{V}}_i$ matrices associated with the eigenvalues,

$$\begin{aligned}\mathbf{W}_N = \bar{\mathbf{V}}_1\mathbf{I}_{k_1}\bar{\mathbf{V}}_1^T + \bar{\mathbf{V}}_2(-\mathbf{I}_{k_2})\bar{\mathbf{V}}_2^T \\ + \bar{\mathbf{V}}_3(j\mathbf{I}_{k_3})\bar{\mathbf{V}}_3^T + \bar{\mathbf{V}}_4(-j\mathbf{I}_{k_4})\bar{\mathbf{V}}_4^T\end{aligned} \quad (15)$$

where $\mathbf{I}_{k_i}$ is $k_i \times k_i$ identity matrix. Actually, $\lambda\mathbf{I}_{k_i}$ can be written explicitly for $\lambda = \{1,-1,j,-j\}$,

$$\begin{aligned}\mathbf{I}_{k_1} &= \text{diag}(e^{-j2\pi(k_1-1)}, ..., e^{-j2\pi}, e^{-j0}) \\ -\mathbf{I}_{k_2} &= \text{diag}(e^{-j\pi+2\pi(k_2-1)}, ..., e^{-j3\pi}, e^{-j\pi}) \\ j\mathbf{I}_{k_3} &= \text{diag}(e^{-j3\pi/2+2\pi(k_3-1)}, ..., e^{-j7\pi/2}, e^{-j3\pi/2}) \\ -j\mathbf{I}_{k_4} &= \text{diag}(e^{-j\pi/2+2\pi(k_4-1)}, ..., e^{-j5\pi/2}, e^{-j\pi/2}).\end{aligned} \quad (16)$$

$\mathbf{I}_{k_i}$ is sorted in a different way compared to (14). The reason of sorting the eigenvalues in the reverse order is concerned with the zero-crossings of the corresponding eigenvectors, which are related to the order of Hermite-type functions. There are n zero-crossings in a Hermite function of order n. Since the zero-crossings in the CDFT matrix is sorted in the order of high to low, e.g. there are no zero-crossings in the middle and there are $N-1$ zero crossings in the first column, we also sort the eigenvalues in the reverse order.

The DFrFT matrix can be obtained by combining (13), (10), and (16) as,

$$\begin{aligned}\mathbf{W}_N^a = \bar{\mathbf{V}}_1\bar{\mathbf{\Lambda}}_{k_1}^a\bar{\mathbf{V}}_1^T + \bar{\mathbf{V}}_2\bar{\mathbf{\Lambda}}_{k_2}^a\bar{\mathbf{V}}_2^T \\ + \bar{\mathbf{V}}_3\bar{\mathbf{\Lambda}}_{k_3}^a\bar{\mathbf{V}}_3^T + \bar{\mathbf{V}}_4\bar{\mathbf{\Lambda}}_{k_4}^a\bar{\mathbf{V}}_4^T\end{aligned} \quad (17)$$

where,

$$\begin{aligned}\bar{\mathbf{\Lambda}}_{k_1}^a &= \text{diag}\left(e^{-j2\pi(k_1-1)a}, \ldots, e^{-j2\pi a}, e^{-j0}\right) \\ \bar{\mathbf{\Lambda}}_{k_2}^a &= \text{diag}\left(e^{-j(\pi+(k_{-1}-1)2\pi)a}, \ldots, e^{-j3\pi a}, e^{-j\pi a}\right) \\ \bar{\mathbf{\Lambda}}_{k_3}^a &= \text{diag}\left(e^{-j(\frac{3\pi}{2}+(k_j-1)2\pi)a}, \ldots, e^{-j\frac{7\pi}{2}a}, e^{-j\frac{3\pi}{2}a}\right) \\ \bar{\mathbf{\Lambda}}_{k_4}^a &= \text{diag}\left(e^{-j(\frac{\pi}{2}+(k_{-j}-1)2\pi)a}, \ldots, e^{-j\frac{5\pi}{2}a}, e^{-j\frac{\pi}{2}a}\right).\end{aligned} \quad (18)$$

As $\bar{\mathbf{V}}_i$ are orthonormal to each other, (17) implies that the index additivity rule is supported, since it can easily be shown that, $\mathbf{W}_N^{a_1}\mathbf{W}_N^{a_2} = \mathbf{W}_N^{a_1+a_2}$. In Section 5, the proposed method is tested on two different scenarios. The aim of the first scenario is to test whether the proposed CDFrFT approximates the samples of its continuous counterpart. The second scenario is to justify the rotation property of the CDFrFT.

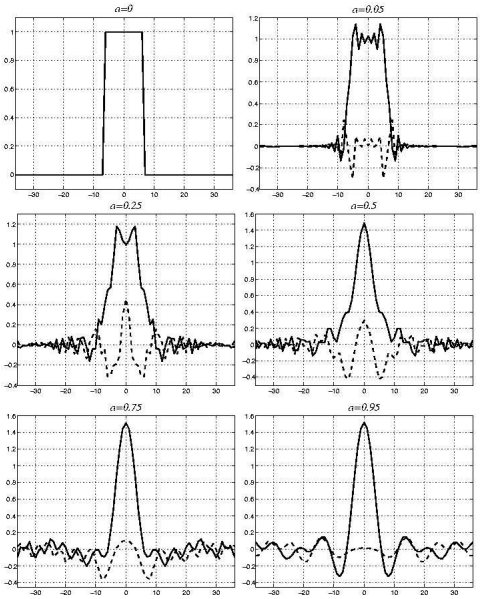

Figure 1: CDFrFT of a discrete rectangular function by the proposed method. $x[n] = 1$ for $-6 \leq n \leq 6$, and x(n) = 0 otherwise. Solid: real part, dashed: imaginary part.

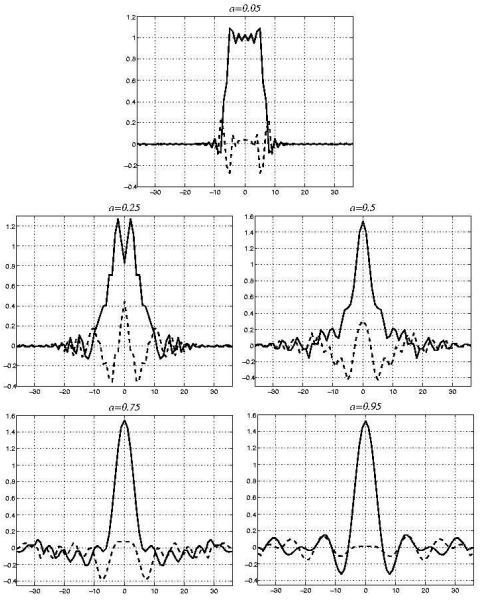

Figure 2: Samples of continuous FrFT of the discrete rectangular function given in Fig. 1.

5. SIMULATIONS AND THE APPLICATION OF CENTERED-DFRFT

In the first scenario, a discrete square function $x[n]$ of length $N = 73$ is generated, where $x[n] = 1$ for $-6 \leq 0 \leq 6$ and $x[n] = 0$ otherwise. The simulation results by the proposed CDFrFT method for various orders are shown in Fig. 1. Fig. 2 shows the samples of the continuous FrFT for the same orders. By comparing the results, it is clear that our proposed method successfully approximates the samples of its continuous counterpart.

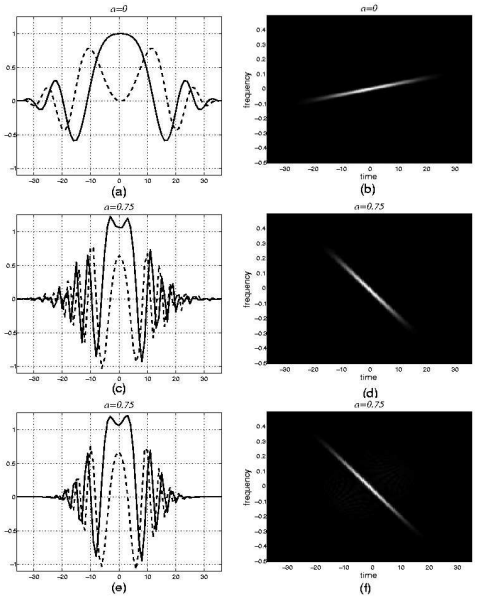

Figure 3: (a) An LFM signal with chirp rate $\beta = 0.1$, (b) its WD, (c) proposed a^{th}-order CDFrFT of the signal, (d) its WD, (e) a^{th}-order FrFT of the signal, and (f) its WD. Solid: real part, dashed: imaginary part.

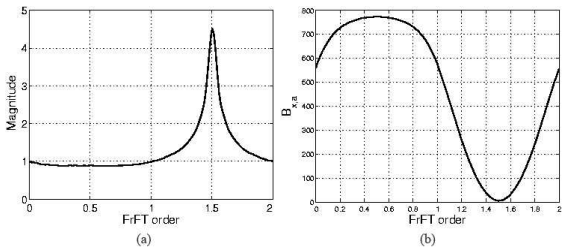

Figure 4: (a) Maximum magnitude of transformed chirp-type signal by CDFrFT with respect to transform order. (b) $B_{x,a}$ versus FrFT order.

The second scenario presents the rotation property of the CDFrFT. A linear frequency modulated (LFM) signal $y[n]$ with a chirp rate of $\beta = 0.1$ is generated with length $N = 73$,

$$y[n] = G[n]exp\left(j\beta n^2\right)$$

where $G[n]$ is the Gaussian envelope of the signal. Fig. 3.(a) presents real and imaginary parts of the signal. WD of the signal is shown in the Fig. 3.(b). The signal is transformed using the proposed CDFrFT with a transform order $a = 0.75$, which is shown in Fig. 3.(c). WD of the obtained signal is in Fig. 3.(d). The samples of the continuous FrFT is plotted in Fig. 3.(e) and its WD is shown in Fig. 3.(f). Compared to the samples of the continuous FrFT, it is obvious that the proposed CDFrFT rotates the axes of the WD successfully by approximating the samples.

As a consequence, our proposed DFrFT has following properties,

- Unitarity. Since the eigenvectors are orthonormal due to the Gram-Schmidt orthogonalization process,
- Index additivity, (see (17), (18)),
- Approximating the samples of the continuous FrFT,

- Reducing to the ordinary DFT when the order $a = 1$,
- Rotating the time-frequency axis by angle $\alpha = a\pi/2$,
- Invertability. Inverse transform of a transformed signal gives exactly the original signal.

5.1 Chirp Rate Estimation by Maximizing the FrFT Magnitude

We have used the CDFrFT to estimate the rate of a chirp signal. For this purpose, a chirp signal is generated with a chirp rate of $\beta_0 = 0.5$. FrFT of the chirp signal gives a dirac-delta-type output at its optimum transform order $a = 1 + \beta_0$ and reaches to a maximum magnitude. Hence, chirp rate of an LFM-type discrete signal $z[n]$ can be estimated by,

$$\hat{a} = \max_a \{\sup(|\mathbf{W}_N^a.z|)\}.$$

Here, $\sup(.)$ determines the peak value of each CDFrFT magnitude and $\hat{a}$ corresponds to the maximum of their suprema. Fig. 4 plots the maximum magnitude versus CDFrFT order a. It is apparent that the proposed CDFrFT gives a peak at the optimum transform order near $\hat{a} = 1.5$. The estimated chirp rate is found to be 1.507 and the error is $7e-3$. The chirp rate estimate $\hat{\beta}_0 = \hat{a} - 1$ is successfully found with a small error rate.

5.2 Chirp Rate Estimation by Fractional Bandwidth Extrema

Frequency-domain bandwidth B_x of a signal $x(t)$ is defined as,

$$B_x = \frac{\left[\int (f-\eta_f)^2 |X(f)|^2\right] \mathrm{d}f}{||x||}, \qquad \eta_f = \frac{\int f|X(f)|^2 \mathrm{d}f}{||x||^2}.$$

where X(f) is the FT of x(t) and $||.||$ is the norm operator. We define the fractional bandwidth of a signal

$$B_{x,a} = \frac{\left[\int (u-\eta_{u,a})^2 |x_a(u)|^2\right] \mathrm{d}u}{||x||}, \quad \eta_{u,a} = \frac{\int u|x_a(u)|^2 \mathrm{d}u}{||x||^2}.$$

Without losing generality, if we take the sampling interval $T_s = 1$, the discrete fractional bandwidth $\tilde{B}_{x,a}$ of a discrete signal $x[n]$ can be defined by,

$$\tilde{B}_{x,a} = \frac{\left[\sum (n-\tilde{\eta}_{n,a})^2 |x_a[n]|^2\right]}{||x||}, \quad \tilde{\eta}_{n,a} = \frac{\sum n|x_a[n]|^2}{||x||^2}.$$

Another method for chirp-rate estimation problem is to find the order that maximizes the fractional bandwidth $\tilde{B}_{x,a}$ of the signal, since a chirp signal is transformed into a sinusoidal at the appropriate FrFT order. The order, which minimizes the bandwidth will maximize the time-width, therefore the order can also be found by maximizing the time-bandwidth ratio. Estimate of the chirp rate can be written as $\hat{\beta} = \max_a\{\tilde{B}_{x,a}\}$, or $\hat{a} = \min_a\{\tilde{B}_{x,a}\}$, where $\hat{a} = 1 + \hat{\beta}$. To minimize the error, mean of the two estimates can be written as,

$$\hat{\tilde{\beta}} = \left(\max_a\{\tilde{B}_{x,a}\} + \min_a\{\tilde{B}_{x,a}\} - 1\right)/2$$

Fig. 4.(b) shows how minimum and maximum fractional bandwidths that are calculated with the CDFrFT are related to chirp-rate. We have found the estimate $\hat{\tilde{\beta}}$ as 1.5069, with an error of $6.9e-3$.

6. CONCLUSIONS

In this work, we have introduced a novel CDFrFT matrix based on a simple and straightforward deduction of eigenvectors from CDFT. The proposed method exhibits high degree of similarity with the properties of the continuous FrFT, such as approximating the samples of the continuous FrFT, reduction to the ordinary CDFT when the transform order $a = 1$, maintaining index additivity rule, being unitary, and possessing rotation property. Simulations and an application on LFM signal parameter estimation problem present that the proposed CDFrFT is a powerful tool for discrete FrFT computation purposes. Future work on this subject may include computation of discrete FrFT based on DFT matrix using appropriate shifting operators in time/frequency and fast computation methods of the proposed transform.

REFERENCES

[1] H. M. Ozaktas, Z. Zalevski, and M. A. Kutay, *The fractional Fourier transform with applications in optics and signal processing* New York:Wiley and Sons, 2001.

[2] L. Durak and O. Arkan, "Short-time Fourier transform: Two fundamental properties and an optimal implementation", *IEEE Trans. on Signal Process.*, vol.51, no.5, pp.1231-1242, 2003.

[3] V. Namias, "The fractional order Fourier transform and its application to quantum mechanics," *J. Inst. Math. Applicat.*, vol. 25, pp. 241–265, 1980.

[4] A. Serbes and L. Durak, "Optimum signal and image recovery by the method of alternating projections in fractional Fourier domains," *Commun. Nonlinear Sci. and Numerical Comput.*, accepted for publication, 2009.

[5] C. D. Luigi and E. Moreau, "An iterative algorithm for estimation of linear frequency modulate signal parameters," *IEEE Signal Process. Lett.*, vol. 9, pp. 127–129, 2002.

[6] M. T. Hanna, N. P. A. Seif and W. A. E. M. Ahmed, "HermiteGaussian-like eigenvectors of the discrete Fourier transform matrix based on the singular-value decomposition of its orthogonal projection matrices," *IEEE Trans. Circ. Syst.-I: Regular Papers*, vol. 51, no. 11, pp. 2245–2254, 2004.

[7] B. W. Dickinson and K. Steiglitz, "Eigenvalues and eigenvectors of the discrete Fourier transform," *IEEE Trans. Acoust. Speech Signal Process.*, vol. 30, no. 1, pp. 25–31, 1982.

[8] S. C. Pei, M. H. Yeh, and C. C. Tseng, "Discrete fractional Fourier transform based on orthogonal projections," *IEEE Trans. Signal Process.*, vol. 47, no. 5, pp. 1335–1348, 1999.

[9] C. Candan, M. A. Kutay, and H. M. Ozaktas, "The discrete fractional Fourier transform," *IEEE Trans. Signal Process.*, vol. 48, no. 5, pp. 1329–1337, 2000.

[10] F. A. Grünbaum, "The eigenvectors of the DFT," *J. Math. Anal. Appl.*, vol. 88, no. 2, pp. 355–363, 1982.

[11] S. C. Pei, V. L. Hsue, and J. J. Ding, "Discrete fractional Fourier transform based on new nearly tridiagonal commuting matrices," *IEEE Trans. Signal Process.*, vol. 54, no. 10, pp. 3815–3828, 2006.

[12] J. G. Vargas-Rubio and B. Santhanam, "On the multiangle centered discrete fractional Fourier transform," *IEEE Signal Process. Lett.*, vol. 12, no. 4, pp. 273-276, 2005.

[13] N. K. Bose, 'Eigenvectors and eigenvalues of 1-D and n-D DFT matrices," *AEU Int. Jour. Electronics and Commun.*, vol. 55, no. 2, pp. 131–133, 2001.

[14] C. D. Meyer, *Matrix analysis and applied linear algebra*. Philadelphia: SIAM Press, 2000.